Circuit Bandwidth Requirements for NRZ and PAM4 Signals

Mahdi Forghani and Behzad Razavi
Electrical and Computer Engineering Department
University of California, Los Angeles, CA, 90095, USA
Emails: forghani@ucla.edu, razavi@ee.ucla.edu

***Abstract*—Wireline links present various circuit stages in the signal path, requiring sufficient bandwidth so as to contribute negligible intersymbol interference. This paper analyzes the effect of circuit bandwidth limitations on NRZ and PAM4 waveforms and quantifies the necessary excess bandwidth when the data format is changed from the former to the latter so as to double the data rate. It is observed that the PAM4 eye width is particularly sensitive, demanding at least a fourfold increase in the bandwidth.**

***Index Terms*—Wireline, PAM4, NRZ, eye diagram.**

I. Introduction

Wireline transceivers typically incorporate NRZ and PAM4 signaling to deal with lossy channels [1–5]. In such an environment, a number of circuits in the signal path must support these data formats with sufficient bandwidth so as to introduce minimal intersymbol interference (ISI). One may surmise that changing the signaling from NRZ to PAM4 to double the data rate simply incurs a factor of 3 reduction in the amplitude but does not otherwise degrade the eye diagram. This paper shows that such an assumption is incorrect and the circuit bandwidth (BW) must be increased significantly for PAM4 signals to avoid additional ISI. This result holds for different types of circuit frequency response.

Section II describes the background for this work and Section III deals with first-order circuits. Section IV extends the study to second-order and T-coil-based stages. Section V repeats the analysis for cascaded stages and Section VI reexamines the results for the case of finite input transition times.

II. Background

Figure 1 shows a typical wireline link, highlighting the interfaces that must support PAM4 waveforms. The transmitter in Fig. 1(a) must achieve a sufficient speed at the DAC output so as to deliver NRZ data at, e.g., 56 Gb/s and PAM4 signals at, e.g., 112 Gb/s. Similarly, the receiver in Fig. 1(b) must guarantee enough bandwidth in the cascade of the variable-gain amplifier (VGA), the continuous-time linear equalizer (CTLE), and the buffer that drives the large number of interleaved channels within the ADC.

We may be tempted to allow some bandwidth limitation in these interfaces and volunteer the CTLE to compensate for it. However, with low supply voltages and nanometer transistors, the boost factor per CTLE stage is quite limited (typically < 6 dB). The issue becomes more severe if the CTLE must provide linear processing for PAM4 signals. In other words, it is generally necessary for the circuits in Fig. 1 to introduce minimal ISI of their own.

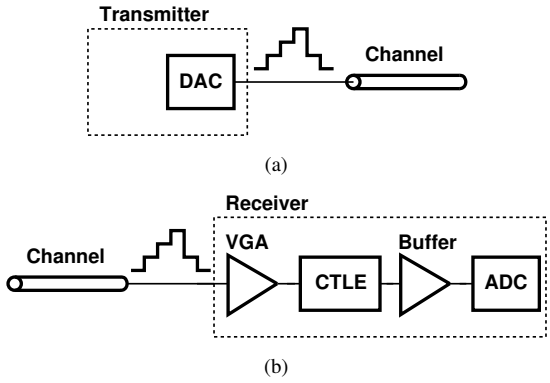

Fig. 1. A typical (a) wireline transmitter and (b) wireline receiver.

The stages shown in Fig. 1 incorporate various broadband techniques such as inductive peaking, T-coil peaking, and negative Miller capacitances [6], exhibiting second- or higher-order responses. We begin our study with a first-order response and then deal with higher-order networks and cascaded stages as well.

III. Bandwidth Requirements for First-Order Circuits

In this section, we calculate the width, W, and height, H, of eye openings for NRZ and PAM4 data travelling through a first-order transfer function. The results provide insight about the additional bandwidth that is necessary if PAM4 waveforms are to replace NRZ signals for doubling the data rate.

A. NRZ Eye

Consider the NRZ waveform, $x(t)$, shown in Fig. 2(a), where, as the worst case, a long run precedes the transition at $t = 0$, and the high level lasts for 1 symbol period, T_S. We denote such a pattern by $x(t) = -A \rightarrow +A \rightarrow -A$. Along with an opposite pattern, $+A \rightarrow -A \rightarrow +A$, this waveform creates the eye diagram $y(t)$. The eye width is computed as $t_b - t_a$ and the eye height as $2y_1$, where t_a and t_b are the zero crossing instants, and y_1 is the output value at the middle of the eye $t = (t_a + t_b)/2$. We should remark that the eye height is, in fact, greatest at $t = t_b$, but the sharp change afterward would make the sampled value sensitive to clock timing.

For a first-order transfer function, $H(s) = 1/(1 + s/\omega_0)$, the time constant is given by $\tau = 1/\omega_0$. For

978-1-6654-8485-5/22/$31.00 ©2022 IEEE

$x(t) = -A \to +A \to -A$, we obtain $t_a = \tau \ln 2$ and $t_b = T_S + \tau \ln\left(2 - 2e^{-T_S/\tau}\right)$, and hence

$$\begin{aligned} W &= t_b - t_a \\ &= T_S + \tau \ln\left(1 - e^{-T_S/\tau}\right). \end{aligned}$$

Also,

$$\begin{aligned} H &= 2y_1 = 2y\left(\frac{t_a + t_b}{2}\right) \\ &= 2\left(1 - \frac{e^{-T_S/(2\tau)}}{\sqrt{1 - e^{-T_S/\tau}}}\right) A. \end{aligned}$$

For a fair comparison of eye openings, H and W are normalized to their ideal values:

$$H_n = 1 - \frac{e^{-T_S/(2\tau)}}{\sqrt{1 - e^{-T_S/\tau}}} \tag{1}$$

$$W_n = 1 + \frac{\tau}{T_S} \ln\left(1 - e^{-T_S/\tau}\right). \tag{2}$$

For example, if the bandwidth is equal to the Nyquist rate, i.e., if $\omega_0/(2\pi) = 0.5/T_S$, then $H_n \approx 0.79$ and $W_n \approx 0.99$, suggesting that the vertical opening is more sensitive to the bandwidth.

B. PAM4 Eye

PAM4 waveforms exhibit 12 types of major and minor transitions. To compute the openings for one of the three eyes, we must determine the worst case, which corresponds to a sequence of $-A \to +A/3 \to -A$ for the middle eye [Fig. 2(b)]. This and the opposite sequence, $+A \to -A/3 \to +A$, yield the smallest eye height and width. For a first-order system, we have

$$H = \frac{2}{3}\left(1 - \frac{e^{-T_S/(2\tau)}}{\sqrt{\frac{1}{3}\left(1 - e^{-T_S/\tau}\right)}}\right) A$$

$$W = T_S + \tau \ln \frac{1 - e^{-T_S/\tau}}{3}.$$

The eye height must be normalized to its nominal value, $2A/3$. It follows that

$$H_n = 1 - \frac{e^{-T_S/(2\tau)}}{\sqrt{\frac{1}{3}\left(1 - e^{-T_S/\tau}\right)}} \tag{3}$$

$$W_n = 1 + \frac{\tau}{T_S} \ln \frac{1 - e^{-T_S/\tau}}{3}. \tag{4}$$

For example, if $\omega_0/(2\pi) = 0.5/T_S$, then $H_n \approx 0.63$ and $W_n \approx 0.64$, revealing significant eye closure. These results also apply to the upper and lower eyes of PAM4.

C. Comparison of NRZ and PAM4 Eyes

Equations (1) and (3) reveal that, for a given τ, H_n is less for PAM4 data than for NRZ signals. Similarly, (2) and (4) indicate greater horizontal closure for PAM4. More generally, we can plot these equations as a function of the circuit bandwidth, arriving at the results depicted in Fig. 3, where we have assumed, as an example, 56-Gb/s NRZ and

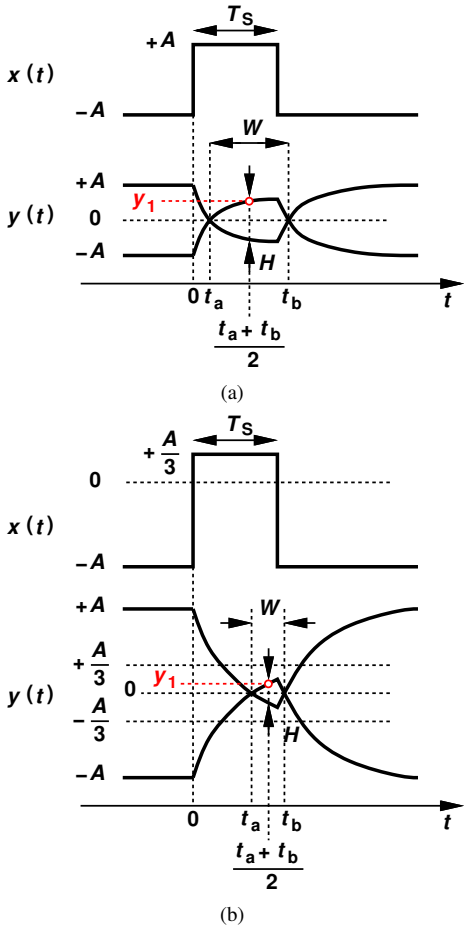

Fig. 2. (a) NRZ eye and (b) PAM4 eye calculations.

112-Gb/s PAM4 signals and simulated a first-order circuit. The key point here is the substantially greater bandwidth required for the latter. For example, an 80% vertical opening demands BW = 29.0 GHz and BW = 38.6 GHz for NRZ and PAM4 circuits, respectively, i.e., a 33% increase. Also, an 80% horizontal opening translates to corresponding bandwidths of 12.5 GHz and 49.1 GHz . We remark that the PAM4 eye width by far dominates the choice of BW. In summary, changing from NRZ to PAM4 data requires a fourfold increase in BW if 80% horizontal openings are desired. We also say the necessary "excess" bandwidth is 300%.

IV. Second-Order and T-Coil-Based Circuits

Shown in Fig. 4 are two common types of stages used in broadband designs [7–10]. We wish to repeat the analysis of the previous section for these circuits and obtain results such as those in Fig. 3.

For the shunt-peaking topology of Fig. 4(a), we assume a damping factor, $\zeta = \sqrt{3}/2$, so that it improves the bandwidth by roughly 60% while incurring minimal overshoot in its step response. Figure 5(a) plots the normalized eye openings. Here, the circuit is designed for different bandwidths by adjusting both C_1 and L_1. We observe that an 80% vertical opening requires 23% more bandwidth for PAM4 data; an 80%

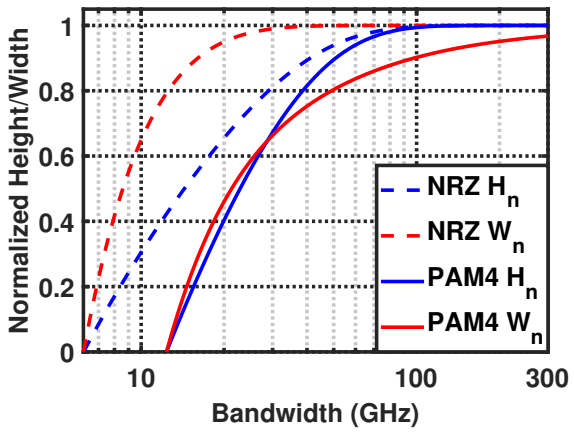

Fig. 3. Normalized eye openings of NRZ at 56 Gb/s and PAM4 at 112 Gb/s vs bandwidth for a first-order system.

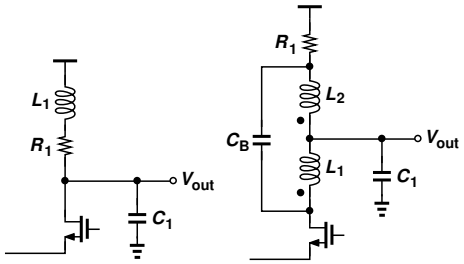

(a) (b)

Fig. 4. Broadband techniques: (a) inductive shunt peaking, (b) t-coil peaking.

horizontal opening dictates 295% more. The latter values is close to that predicted by the first-order model in Section III.

It is important to note that PAM4 eyes are more sensitive to the value of ζ: some overshoot in an underdamped response proves fairly benign to NRZ data, but reduces the vertical opening in PAM4 signals.

The T-coil-based stage of Fig. 4(b) is analyzed in a similar manner, with $\zeta = \sqrt{3}/2$ for optimal response [11]. To plot the eye openings as a function of the circuit's bandwidth, we adjust C_1, L_1, L_2, and C_B while maintaining a mutual coupling factor, k, equal to 0.5 for ease of implementation [11]. From these simulations emerge the plots in Fig. 5(b), suggesting that for 80% vertical or horizontal openings, PAM4 waveforms demand an excess bandwidths of 24% and 304%, respectively. Figure 6 depicts the simulated eye diagrams for this case.

V. Cascaded Stages

The transfer functions related to the DAC output node in Fig. 1(a) and the VGA, the CTLE, and the buffer in Fig. 1(b) are equivalently multiplied. We can therefore ask how NRZ and PAM4 signals behave in cascaded circuits. We consider cascades consisting of two identical stages, each stage having a first-order, second-order, or T-coil-based response.

Figure 7 plots the results obtained from circuit simulations, where the cascade bandwidth is varied and the eye openings are measured. We observe that, as far as W_n is concerned,

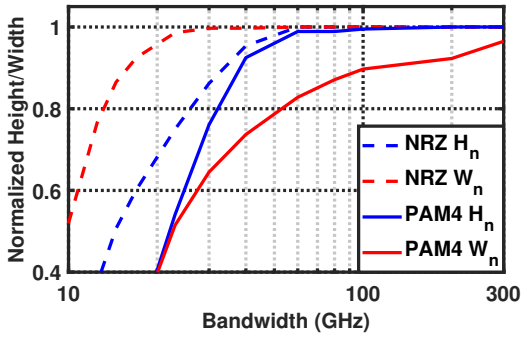

(a)

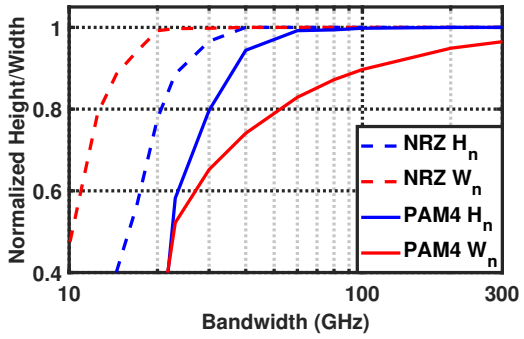

(b)

Fig. 5. Normalized eye openings of NRZ at 56 Gb/s and PAM4 at 112 Gb/s vs bandwidth for (a) second-order circuit (shunt peaking), and (b) T-coil-based circuit.

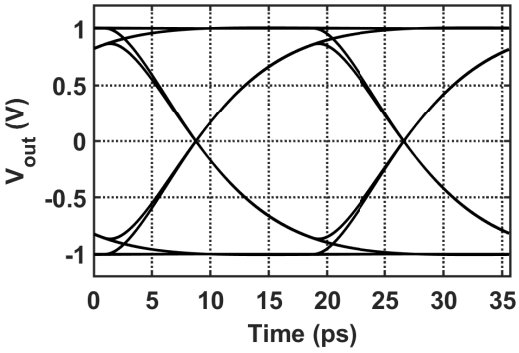

(a)

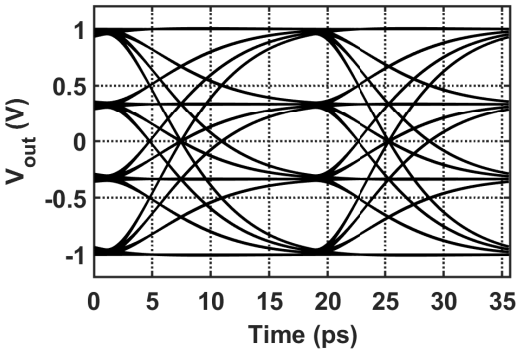

(b)

Fig. 6. Output eye diagrams for (a) NRZ and (b) PAM4 data with H_n=80% in T-coil-based stages.

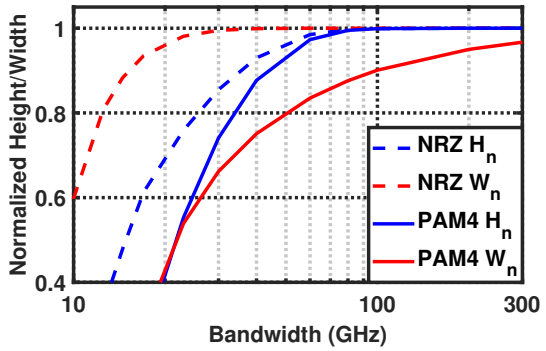

(a)

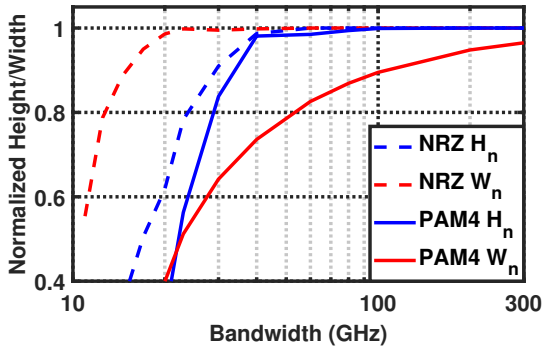

(b)

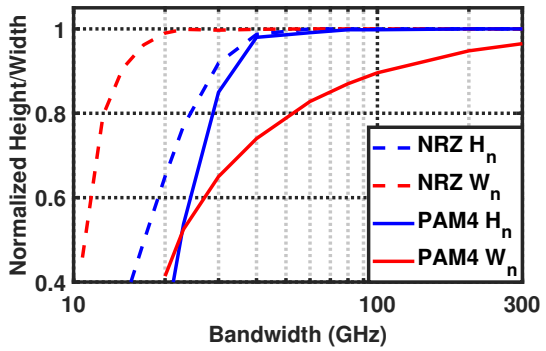

(c)

Fig. 7. Normalized eye openings of NRZ at 56 Gb/s and PAM4 at 112 Gb/s vs bandwidth (a) cascaded first-order stages, (b) cascaded second-order stages, (c) cascaded T-coil-based stages.

cascading further intensifies the required bandwidth disparity between NRZ and PAM4 waveforms; for 80% openings, the excess bandwidth reaches 314%.

VI. Effect of Finite Transition Times

The analyses performed in the previous sections have assumed zero rise and fall times for the input NRZ and PAM4 data. In reality, these times are bounded by the bandwidth of the preceding stage. For example, the DAC in Fig. 1(a) receives its MSB and LSB NRZ data from multiplexers at a rate of 56 Gb/s. We expect the rise and fall times to be on the order of 6 ps in this example and wish to repeat the foregoing calculations for first-order, second-order, T-coil-based, and cascaded stages.

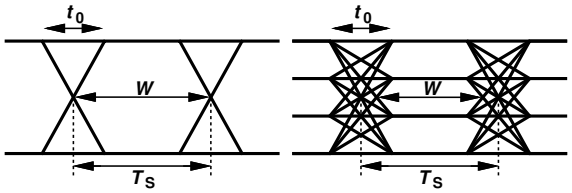

(a) (b)

Fig. 8. Effect of rise and fall time on the (a) NRZ eye, (b) PAM4 eye.

One can readily appreciate the PAM4 eye closure with a finite transition time of t_0. As shown in Fig. 8 for infinite bandwidth, the NRZ normalized width remains unchanged whereas the PAM4 width drops to

$$W_{n,\max} = 1 - \frac{t_0}{2T_S}.$$

For the sake of brevity, we summarize all of the simulation results for 80% eye openings in Fig. 9. These results offer a number of insights. First, approximation of circuits by first-order networks overestimates the necessary bandwidth increase for H_n but provides a reasonable estimate for W_n. Second, for nonzero transition times, maintaining $W_n \approx 80\%$ raises the excess BW from 300% to nearly 450% (i.e., by a factor of 5.5). Third, for a given overall bandwidth, single-stage and two-stage circuits impose roughly the same excess bandwidth requirements for PAM4.

VII. Conclusion

This paper analyzes the necessary excess bandwidth in circuits that process NRZ signals at a certain data rate or PAM4 waveforms at twice that rate. Different types of frequency response are studied, and it is shown that the bandwidth must increase considerably for the latter.

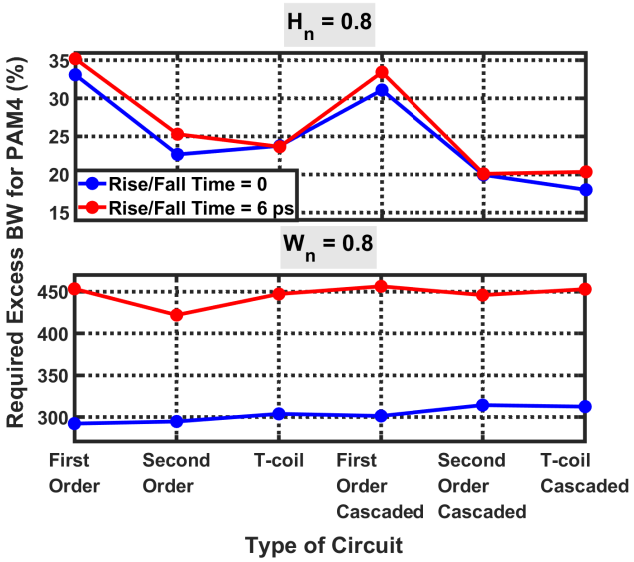

Fig. 9. Required excess BW for PAM4 with 80% eye openings with zero or 6-ps rise and fall times.

ACKNOWLEDGMENT

This research is supported by Realtek Semiconductor.

REFERENCES

[1] P. Upadhyaya *et al.*, "A fully adaptive 19-to-56 Gb/s PAM-4 wireline transceiver with a configurable ADC in 16nm FinFET," in *IEEE ISSCC Dig. Tech. Papers*, Feb. 2018, pp. 108–110.

[2] J. Im *et al.*, "A 112-Gb/s PAM-4 long-reach wireline transceiver using a 36-way time-interleaved SAR ADC and inverter-Based RX analog front-end in 7-nm FinFET," *IEEE J. Solid-State Circuits*, vol. 56, no. 1, pp. 7–18, Jan. 2021.

[3] P.-J. Peng, J.-F. Li, L.-Y. Chen, and J. Lee, "A 56Gb/s PAM-4/NRZ transceiver in 40nm CMOS," in *IEEE ISSCC Dig. Tech. Papers*, Feb. 2017, pp. 110–111.

[4] J. Han, N. Sutardja, Y. Lu, and E. Alon, "Design techniques for a 60-Gb/s 288-mW NRZ transceiver with adaptive equalization and baud-rate clock and data recovery in 65-nm CMOS technology," *IEEE J. Solid-State Circuits*, vol. 52, no. 12, pp. 3474–3485, Dec. 2017.

[5] J. Kim *et al.*, "A 224Gb/s DAC-based PAM-4 transmitter with 8-tap FFE in 10nm CMOS," in *IEEE ISSCC Dig. Tech. Papers*, vol. 64, Feb. 2021, pp. 126–128.

[6] S. Galal and B. Razavi, "10-Gb/s limiting amplifier and laser/modulator driver in 0.18 μm CMOS technology," in *IEEE ISSCC Dig. Tech. Papers*, Feb. 2003, pp. 188–487 vol.1.

[7] J. Paramesh and D. J. Allstot, "Analysis of the bridged T-coil circuit using the extra-element theorem," *IEEE Trans. Circuits Syst. II, Exp. Briefs*, vol. 53, no. 12, pp. 1408–1412, Dec. 2006.

[8] S. Shekhar, J. Walling, and D. Allstot, "Bandwidth extension techniques for CMOS amplifiers," *IEEE J. Solid-State Circuits*, vol. 41, no. 11, pp. 2424–2439, Nov. 2006.

[9] J. Kim, J.-K. Kim, B.-J. Lee, and D.-K. Jeong, "Design optimization of On-Chip inductive peaking structures for 0.13-μm CMOS 40-Gb/s transmitter circuits," *IEEE Trans. Circuits Syst. I, Reg. Papers*, vol. 56, no. 12, pp. 2544–2555, Dec. 2009.

[10] N. Zhou, L. Wu, Z. Wang, X. Zheng, W. Cao, C. Zhang, F. Li, and Z. Wang, "A 28-Gb/s transmitter with 3-tap FFE and T-coil enhanced terminal in 65-nm CMOS technology," in *Proc. 14th IEEE Int. New Circuits Syst. Conf. (NEWCAS)*, Jun. 2016, pp. 1–4.

[11] S. Galal and B. Razavi, "Broadband ESD protection circuits in CMOS technology," *IEEE J. Solid-State Circuits*, vol. 38, no. 12, pp. 2334–2340, Dec. 2003.